

LPT 97-05  
 KFA-IKP(TH)-1997-10  
 Coimbra University 260597

MAY 1997

## Quark-antiquark resonances in the NJL model<sup>#1</sup>

Véronique Bernard

*Laboratoire de Physique Théorique, Université Louis Pasteur  
 BP 28, F-67037 Strasbourg Cedex 2, France*

Alex H. Blin, Brigitte Hiller

*Centro de Física Teórica, Departamento de Física  
 da Universidade de Coimbra, P-3000 Coimbra, Portugal*

Yuri P. Ivanov, Alexander A. Osipov

*Joint Institute for Nuclear Research, Laboratory of Nuclear Problems  
 141980 Dubna, Moscow Region, Russia*

Ulf-G. Meißner

*Forschungszentrum Jülich, Institut für Kernphysik (Theorie)  
 D-52425 Jülich, Germany*

### Abstract

The problem of the  $\rho$  meson resonance solution in the extended NJL model is studied. It has been shown previously that the solution for the  $\rho$  meson changes smoothly from a bound state to a “virtual state” when the vector channel attraction becomes too weak to support bound state solutions. We have found that together with these solutions a separate resonance branch appears which is not connected smoothly with the bound state solutions. At small values of constituent quark mass,  $m \sim 200$  MeV, it corresponds to the physical vector meson resonance solution in the quark-continuum region. The  $a_1$  and  $\sigma$  resonances are also discussed.

---

<sup>#1</sup> Supported in part by the grants PCERN /FIS/1034/95, PESO/S/PRO/1057/95, PRAXIS XXI/BCC/7301/96, and JNICT.

1. We have become accustomed to think of resonance states in the extended Nambu–Jona-Lasinio (NJL) model [1] as being solutions of the corresponding Bethe-Salpeter (BS) equations, analytically continued into the complex  $p^2$ -plane. This follows from our quantum mechanical experience in describing a system which can disintegrate. Such a system can have a very small disintegration probability and is then known as a quasi-stationary or a resonance state. The propagator of a quasi-stationary state has always poles in the complex  $p_0$ -plane which are situated close to the real axis. This method can also be applied to systems with a relatively large disintegration probability. Conceivably, we deal with such a kind of states in the case of the strongly interacting quark-antiquark systems in the extended NJL model, if they are located in the continuum region [2].

The question of the location of a complex pole which is close to the real axis can actually be resolved without going in the complex  $p^2$  plane. In this letter we show how to do that. This simple procedure is quite general and can be used whenever one is interested in narrow resonance solutions of a known propagator or self-energy function of the corresponding state. The idea to find out the resonance parameters without going into the complex  $p^2$  plane has been used in the spectral-function (SF) method [3]-[5]. It has been assumed that a maximum in the imaginary part of a meson propagator can be associated with a resonance mass. This approach has been criticized in [6]. It was argued there that although the SF method and the analytical continuation of the BS equations into the complex  $p^2$  plane yield similar results for the  $a_1$  meson, the same methods lead to qualitatively different descriptions in the case of the  $\rho$  meson. Using our approach it is not difficult to understand why the SF method under certain circumstance may lead to wrong conclusions.

There are several reasons why the resonance solutions in a quark continuum region are important. First, the  $a_1$  meson always lies above the  $q\bar{q}$  threshold. Second, the  $\sigma$  meson is displaced in that region when the current quark mass is different from zero. Furthermore, the statement that there is no resonance solution for the  $\rho$  meson [2, 6] requires further investigation. In fact, it can not be excluded that for solutions of the relativistic BS equation there exists a similar difference in the behaviour of  $s$ - and higher partial waves as it is the case in nonrelativistic potential theory. However, it is conceivable that the relativistic BS equation exhibits some new features in comparison with a nonrelativistic theory. In this letter we will show that besides the bound and “virtual state” [6] solutions, which are smoothly connected at some value of the vector interaction strength  $G_V$ , there exists for all values of  $G_V$  a resonance branch for the  $\rho$ -meson. We show that an overall fit to empirical data can be achieved either with large constituent quark masses ( $\sim 400$  MeV) [7] or small ones ( $\sim 200$  MeV). In the former case the physical  $\rho$  meson appears as a bound  $q\bar{q}$  state. The resonance solution corresponds to the physical  $\rho$  meson for small constituent quark masses. This finding lends credit to the approaches which use small values of non-strange quark masses  $m$ , i.e. when  $m_\rho > 2m$ , as it is frequently used in the literature [8]. It also shows that even so in the NJL model confinement is absent, one can still investigate some properties of states which a priori seem to lie outside the range of applicability of the model.

2. Let the propagator of some state be defined by

$$\Delta(p^2) = f^{-1}(p^2) . \quad (1)$$

It frequently happens that the function  $f(p^2)$  becomes complex-valued for certain values of external momenta, and it is thus conceivable that the pole will be displaced into the complex  $p_0$ -plane. One assumes usually that near the pole the propagator behaves as

$$\Delta(p^2) \sim \frac{Z^{-1}}{p^2 - M^2 + i\gamma}, \quad Z = \left( \frac{\partial f(p^2)}{\partial p^2} \right)_{p^2=M^2-i\gamma} \quad (2)$$

where  $\gamma$  is positive, so that for infinitesimal small  $\gamma$  we make contact with the standard  $i\epsilon$  prescription for the propagator poles. In this case the complex pole coordinates  $p^2 = M^2 - i\gamma$  are interpreted as a mass,  $M$ , and a width,  $\Gamma = \gamma/\omega(\mathbf{p})$ , of a corresponding resonance state. Here  $\omega(\mathbf{p}) = \sqrt{(\mathbf{p}^2 + M^2)}$  is an energy. This interpretation follows from the fact that the leading contribution of the Fourier-transformed two-point function at large time originates from the momenta associated with the propagator pole in the lower complex  $p_0$ -plane.

If  $\gamma$  is small ( $\gamma \ll M^2$ ) the equation  $f(M^2 - i\gamma) = 0$  can be solved in the small width approximation, that is by expanding it around the point  $M^2 - i0$  in a Taylor series and restricting oneself to the terms linear in  $\gamma$ . This is possible if the function  $f$  is analytic everywhere inside a circle  $\mathcal{C}_0$  with center at  $M^2 - i0$  and  $M^2 - i\gamma \in \mathcal{C}_0$ . We assume that the branch cut of  $f$  does not pass the circle  $\mathcal{C}_0$ . In this case one obtains

$$\gamma = \frac{I_f}{R'_f}, \quad R_f R'_f + I_f I'_f = 0, \quad (3)$$

where

$$\begin{aligned} R_f &= \operatorname{Re} f(p^2), & I_f &= \operatorname{Im} f(p^2), \\ R'_f &= \frac{\partial \operatorname{Re} f(p^2)}{\partial p^2}, & I'_f &= \frac{\partial \operatorname{Im} f(p^2)}{\partial p^2}, \end{aligned} \quad (4)$$

taken at  $p^2 = M^2$ . Solving the second equation in (3) one can obtain the mass and the first one gives the width. It is, however, mandatory to check that the self-consistency requirement  $\gamma \ll M^2$  is fulfilled.

3. One can arrive at the equations (3) without going into the complex  $p^2$  plane. Consider only real values of momenta. We look for a point  $q^2$  on the real  $p^2$ -axis such that in the neighbourhood of it the function  $f(p^2)$  can be written in the form  $f(p^2) \approx Z_0(p^2 - q^2 + i\gamma) + \mathcal{O}(p^2 - q^2)$ . The function  $f(p^2)$  can be expanded around some close-by but arbitrary point  $q^2$ ,

$$f(p^2) = \operatorname{Re} f(q^2) + i\operatorname{Im} f(q^2) + (p^2 - q^2) \left[ \frac{\partial \operatorname{Re} f(p^2)}{\partial p^2} + i \frac{\partial \operatorname{Im} f(p^2)}{\partial p^2} \right]_{p^2=q^2} + \dots \quad (5)$$

The ellipses indicate terms of higher order in  $(p^2 - q^2)$ . It follows that

$$f(p^2) = Z_0[p^2 - q^2(1 - \lambda) + i\gamma] + \dots \quad (6)$$

where  $\gamma$ ,  $\lambda$  and  $Z_0$  are given by

$$\gamma(q^2) = \frac{I_f R'_f - R_f I'_f}{(R'_f)^2 + (I'_f)^2}, \quad (7)$$

$$\lambda(q^2) = \frac{R_f R'_f + I_f I'_f}{q^2[(R'_f)^2 + (I'_f)^2]}, \quad (8)$$

$$Z_0 = \left( \frac{\partial f(p^2)}{\partial p^2} \right)_{p^2=q^2}. \quad (9)$$

Thus, if  $\lambda(q^2)$  is equal to zero one can identify the corresponding value of  $q^2$  with the mass of the resonance state and obtain the width of this state from Eq.(7). Indeed, if  $\lambda(q^2) = 0$  the equality  $R_f R'_f + I_f I'_f = 0$  is fulfilled. Inserting it in the expression for  $\gamma$  and using that now  $I_f R'_f - R_f I'_f = [(R'_f)^2 + (I'_f)^2] I_f / R'_f$ , we obtain a result fully coinciding with Eqs.(3). This shows that when the points  $q^2$  and  $q^2 - i\gamma$  are close to each other an approach with the self-consistency condition in the form

$$\lambda(q^2) = 0 \quad (10)$$

is equivalent to the method of the complex pole in the small width approximation. Actually, it is a simple consequence of the fact that the derivative of an analytic function  $f(z)$  at the point  $z_0$  does not depend on the way which the point  $z_0$  has been approached. In particular, it does not matter from which direction we calculate the value  $f'(p^2)$  to obtain the result Eqs.(3), whether along the real axis or along the imaginary one. The manner in which we have arrived at the formula Eq.(10) is not restricted by the requirement  $\gamma \ll q^2$ . It is clear, however, that at large values of  $\gamma$ , ( $\gamma \sim q^2$ ), the relation of this solution with a complex pole location is not so direct. We conclude that in such type of approach, the function  $\lambda$  plays the crucial role to find a resonance state or to exclude it.

In the case in which the function  $f(p^2)$  is real, it is simple to see that  $\lambda = R_f / (q^2 R'_f)$  and the self-consistency requirement leads to  $R_f = 0$ . This is a well known fact that the mass of physical particles in quantum field theory is associated with the pole of the full propagator.

**4.** Let us consider now the spectral-function method [3]-[5]. The spectral function is the imaginary part of the propagator  $\Delta(p^2)$

$$\xi(p) = \text{Im} \Delta(p^2) = \frac{-I_f}{R_f^2 + I_f^2}. \quad (11)$$

In this approach it is assumed that the parameters of the resonance can be determined from the extremum of the function  $\xi(p)$ . The extremum condition is given by

$$(R_f^2 - I_f^2) I'_f - 2 R_f I_f R'_f = 0 \quad (12)$$

By use of Eqs.(7) and (8) this condition can be written as

$$\lambda(q^2) + \frac{R_f(q^2)}{I_f(q^2)} \left( \frac{\gamma(q^2)}{q^2} \right) = 0 \quad . \quad (13)$$

It is obvious that this criterium is different from the requirement Eq.(10). Therefore, one must be fully aware that in the SF approach there is no direct relation with the complex pole method and from this point of view can lead to incorrect results. This is in fact, very easily understandable. The difference between approaches 2 and 3 and the SF approach comes from the fact that in the SF approach one assumes that  $Z$  is real. Only in that case is the  $\text{Im } \Delta$ , Eq.(2), maximum at  $p^2 = M^2$ . Indeed if  $I'_f = 0$  then Eqs.(13) and (10) are identical. The origin of a complex  $Z$  factor comes from the appearance of a background term in the  $T$  matrix so that a difference between different approaches signals the presence of a non-negligible background. Whenever this happens it is useful to check the determination of the resonance parameters via the speed plot technique [9].

**5.** Consider now an extended NJL model with spin-1 mesons [10, 11]<sup>#2</sup>. For the moment, let us postpone the rigorous solution of the mass equations and content ourselves to discuss the simplest approach to the problem as outlined in section 3. We look for the resonance solutions for vector  $\rho$ , axial vector  $a_1$  and scalar  $\sigma$  mesons, on the basis of Eqs.(3). The corresponding self-energy functions can be written

$$f_\rho(p^2) = \frac{3}{8G_V} - p^2 J_2(p^2), \quad (14)$$

$$f_{a_1}(p^2) = \frac{3}{8G_V} + 6m^2 I_2(p^2) - p^2 J_2(p^2), \quad (15)$$

$$f_\sigma(p^2) = \frac{\widehat{m}}{4mG_S} + (4m^2 - p^2) I_2(p^2) \quad . \quad (16)$$

Here,  $G_V$  and  $G_S$  are the constants of the four-quark interaction of the vector,  $V$ , and the scalar,  $S$ , sectors. We also use the symbols  $\widehat{m}$  and  $m$  for the current and constituent quark masses, respectively. The quark-loop integrals  $I_2$  and  $J_2$  are defined as

$$I_2(p^2) = \frac{N_c}{16\pi^2} \int_0^1 dy \int_0^\infty \frac{dz}{z} R(z) e^{\frac{i}{4} z p^2 (1-y^2)}, \quad (17)$$

$$J_2(p^2) = \frac{3N_c}{32\pi^2} \int_0^1 dy (1-y^2) \int_0^\infty \frac{dz}{z} R(z) e^{\frac{i}{4} z p^2 (1-y^2)}. \quad (18)$$

The Pauli-Villars regulator  $R(z)$  [12] is chosen in the form

$$R(z) = \left[ 1 - (1 + iz\Lambda^2) e^{-iz\Lambda^2} \right] e^{-im^2 z} \quad . \quad (19)$$

It corresponds to two covariant subtractions at large momenta  $p^2 = \Lambda^2 \gg m^2$  leading to a finite result for the  $\rho$ ,  $a_1$  and  $\sigma$  self-energy diagrams. The first two of them contain the

---

<sup>#2</sup>Other references can be found in [11]. We shall follow the notations of that paper here.

quadratically divergent integrals. Using the Pauli-Villars method one can avoid these  $\Lambda^2$  terms from the self-energy diagrams. The following properties of the function  $R(z)$  are important for that:  $R(0) = R'(0) = 0$ .

Evaluating the  $I_2$  and  $J_2$  integrals we get

$$I_2(p^2) = \frac{3}{16\pi^2} \left\{ \ln \left( \frac{\Lambda^2 + m^2}{m^2} \right) + 2 [J(\bar{\xi}) - J(\xi)] + \left( \frac{\Lambda^2}{\Lambda^2 + m^2} \right) \frac{J(\bar{\xi})}{(\bar{\xi} - 1)} \right\} . \quad (20)$$

$$\begin{aligned} J_2(p^2) &= \frac{3}{16\pi^2} \left[ \ln \left( \frac{\Lambda^2 + m^2}{m^2} \right) + \left( 2 + \frac{1}{\bar{\xi}} \right) J(\bar{\xi}) - \left( 2 + \frac{1}{\xi} \right) J(\xi) + \right. \\ &\quad \left. + \frac{1}{2\bar{\xi}} \left( \frac{\Lambda^2}{\Lambda^2 + m^2} \right) \left( 1 + 3 \frac{J(\bar{\xi})}{\bar{\xi} - 1} \right) \right] . \end{aligned} \quad (21)$$

Here

$$\xi = \frac{p^2}{4m^2}, \quad \bar{\xi} = \frac{p^2}{4(\Lambda^2 + m^2)} , \quad (22)$$

and the one-loop function  $J(x)$  of the real variable  $x$  is equal to

$$J(x) = \begin{cases} \frac{1}{2} \sqrt{1 - \frac{1}{x}} \ln \left( \frac{1 + \sqrt{1 - \frac{1}{x}}}{-1 + \sqrt{1 - \frac{1}{x}}} \right) & \text{if } x < 0 , \\ \sqrt{\frac{1}{x} - 1} \arctan \frac{1}{\sqrt{\frac{1}{x} - 1}} & \text{if } 0 < x < 1 . \end{cases} \quad (23)$$

We remark that our function  $J_2(p^2)$  coincides with the corresponding expression from [6], precisely we have  $16\pi^2 p^2 J_2(p^2) = 9\Lambda^2 I_1(z)$ , where  $I_1(z)$  is given by Eq.(15) in [6].

Let us fix the parameters of the model. There are four of them in all:  $G_S, G_V, m$  and  $\Lambda$ . The constituent quark mass,  $m$ , is related to the current quark mass,  $\widehat{m}$ , by the gap equation of the model. We fix parameters of the model in order to obtain the pion decay constant,  $f_\pi$ , and the pion mass,  $m_\pi$ , close to their physical values,  $f_\pi \simeq 93$  MeV and  $m_\pi \simeq 139$  MeV, respectively. The other two input values are determined from the vector mesons sector such that one obtains values close to the empirical masses of  $\rho$ ,  $m_\rho \simeq 770$  MeV and  $a_1$  meson,  $m_{a_1} \simeq 1100$  MeV. We investigate two cases, one with a large constituent quark mass ( $m = 390$  MeV) leading to a bound state solution for the  $\rho$  meson, and one with a small quark mass ( $m = 180$  MeV), where the physical  $\rho$  meson appears as a resonant state in the  $q\bar{q}$ -continuum. We obtain for the large quark mass case:  $G_S = 9.41 \text{ GeV}^{-2}$ ,  $G_V = 10.27 \text{ GeV}^{-2}$ ,  $\widehat{m} = 3.9$  MeV and  $\Lambda = 1$  GeV. With these parameters, we find  $f_\pi = 93.3$  MeV,  $m_\pi = 139$  MeV,  $m_\rho = 776$  MeV,  $m_{a_1} = 1042 - i358$  MeV,  $m_\sigma = 439 - i0.28$  MeV. For the small quark mass case we get:  $G_S = 0.86 \text{ GeV}^{-2}$ ,  $G_V = 6.65 \text{ GeV}^{-2}$ ,  $\widehat{m} = 1$  MeV and  $\Lambda = 2.8$  GeV. With these parameters, we have  $f_\pi = 93.3$  MeV,  $m_\pi = 139$  MeV,  $m_\rho = 674 - i300$  MeV,  $m_{a_1} = 802 - i289$  MeV,  $m_\sigma = 378 - i2.6$  MeV. Note that to determine these resonance properties, we have made use of Eqs.(3).

**6.** In order to search for resonances which lie in the complex plane on the second Riemann sheet, we introduce the following analytic continuation of the functions  $J(\xi)$  and  $J(\bar{\xi})$ .

The function  $J(\xi)$  has a branch point  $P_0$  at  $z = 1$  and a cut along the real axis from  $P_0$  to  $+\infty$ . Analytically continuing this function on the second Riemann sheet we obtain the following analytic function  $\mathcal{F}_0(z)$ , where  $z \in \mathbf{C}$ ,

$$\mathcal{F}_0(z) = \frac{1}{2} \sqrt{1 - \frac{1}{z}} \left[ -i\pi + \log \left( \frac{1 + \sqrt{1 - \frac{1}{z}}}{1 - \sqrt{1 - \frac{1}{z}}} \right) \right] . \quad (24)$$

We are looking for resonances whose masses are smaller than the cut-off  $\Lambda$  so that one does not cross the cut of the function  $J(\bar{\xi})$  which lies from  $P_1$  to  $+\infty$  where  $P_1$  is at  $\bar{z} = 1$ , that is at  $z = 1 + (\Lambda^2/m^2)$ . This function is thus given in the complex plane  $\mathbf{C}$  by the analytic function  $\mathcal{F}_1(\bar{z})$

$$\mathcal{F}_1(\bar{z}) = \frac{1}{2} \sqrt{1 - \frac{1}{\bar{z}}} \log \left( \frac{1 + \sqrt{1 - \frac{1}{\bar{z}}}}{-1 + \sqrt{1 - \frac{1}{\bar{z}}}} \right) , \quad (25)$$

where  $\bar{z} \equiv zm^2/(\Lambda^2 + m^2)$ . Let us consider now the mass equations

$$f_\alpha(z) = 0, \quad \alpha = \sigma, a_1, \rho . \quad (26)$$

It is known<sup>#3</sup> that in the case of  $\sigma$  or  $a_1$  mesons there exists only the resonance solution of these equations. To show them we shall plot functions  $\omega_\alpha(G_V)$  and in some cases also  $\eta_\alpha(G_V)$ , where  $(\omega_\alpha - i\eta_\alpha)^2 = 4m^2 z_\alpha$  and  $z_\alpha$  is a solution of the corresponding equation in Eq.(26) at some value  $G_V$ . We shall call these functions a resonance branch of Eq.(26) if they are a mapping of resonance solutions of this equation at different values of  $G_V$ . The corresponding formulae are

$$\omega_\alpha = mK_\alpha, \quad \eta_\alpha = -2mK_\alpha^{-1} \text{Im} z_\alpha, \quad K_\alpha = \sqrt{\text{Re} z_\alpha + |z_\alpha|}. \quad (27)$$

By our definition  $z$  is proportional to the complex  $p^2$ . In turn complex  $p^2$  reads  $p^2 = (p_0 - i\eta'/2)^2 - \mathbf{p}^2$ . In the rest frame  $\mathbf{p} = 0$  and then  $p^2 = (M - i\eta/2)^2$ . Thus  $\omega$  has a meaning of mass and  $\eta$  is related to the width of the resonance state. If  $\eta$  is small one has  $p^2 = M^2 - i\gamma$ , where  $\gamma = M\eta$ . We used this fact in paragraph 2.

We plot resonance branches for  $\rho$  and  $a_1$  mesons in Figs.1-2 for two different values of quark masses:  $m = 390$  MeV and  $m = 180$  MeV, using the same set of parameters  $(\widehat{m}, m_\pi, \Lambda)$  as in section 5 and varying  $G_V$ . Notice that in the case of the  $\rho$  meson only the bound state branch has been known until now. At  $p^2 > 4m^2$  this curve smoothly transforms into a “virtual state” section. This has been first observed in [6]. In nonrelativistic scattering theory, the appearance of a “virtual state” is directly related to the absence of a near-threshold resonance in the  $s$ -wave. In the relativistic theory, as we have found here by studying the NJL model, the resonance branch appears together with a bound state–“virtual state” branch as a separate curve. It is never smoothly connected with the bound state branch and it has rather large values of the imaginary part  $\eta_\rho$ . For large values of quark mass  $m \sim 400$  MeV (see Fig.1) the  $\rho$  meson solution belongs to the

---

<sup>#3</sup>One can also prove this fact analytically.

bound state branch. However, at relatively small values,  $m \sim 200$  MeV, as one can see from Fig.2, the  $\rho$  meson solution is a resonance state in the quark–antiquark continuum.

We plot in Figs.1-2 only the real parts,  $\omega_\alpha$ , of resonance solutions  $m_\alpha = \omega_\alpha - i\eta_\alpha$ . Therefore the intersection of the resonance branch with the “virtual state” in Figs.1-2 is only a result of this projection on the real  $m_\alpha$  axis. Really the crossing curves have different imaginary parts  $\eta_\alpha$  in these points. We draw them in Figs.3-4. For  $m = 390$  MeV we obtain for the empirical value of  $f_\pi = 93.3$  MeV the  $\rho$ -meson bound state mass  $m_\rho = 776$  MeV and the complex mass for  $a_1$ ,  $m_{a_1} = 1000 - i263$  MeV. For  $m = 180$  MeV, the complex masses of resonance states which correspond to the empirical value of  $f_\pi = 93.3$  MeV are  $m_\rho = 674 - i292$  MeV, and  $m_{a_1} = 802 - i289$  MeV. These values are a bit smaller than the experimental ones. To clarify the  $f_\pi$  dependence of the result we indicate in Figs.1-2 boxes inside which the  $f_\pi$  value changes from  $f_\pi = 100$  MeV on the left side to  $f_\pi = 92$  MeV on their right side. The physical solutions lie inside this box. In the other figures we directly plot  $f_\pi$  as a function of  $G_V$ . As discussed in section 4, we have also checked our results via the speed plot technique. Very good agreement between the two methods was obtained.

It is also interesting to compare the results of the exact solutions of the complex BS equation for the  $\rho$  and the  $a_1$  with the approximate estimations of section 5 (see Figs.3-4). We start the comparison for the case of a large quark mass  $m = 390$  MeV in Fig.3. As one can see the expansion approach works quite well for the  $a_1$  meson. The deviation in the results of the two approaches is smaller at higher values of  $G_V$  where  $\eta_{a_1}$  is smaller as it should be expected. We also plot here the  $\eta_\rho$  values. It follows from section 3 that at  $p^2 < 4m^2$ , Eqs.(3) describe a bound state branch. At large values of the quark mass, we have  $\text{Re}(z_\rho) \ll 1$ , far away from the region of applicability of Eqs.(3) to resonance solutions. The resonance branch as an approximate solution cannot be found in this case. The physical branch for  $\rho$  is a bound state solution, for which the exact solution fully coincides with the solution of Eqs.(3). In Figs. 4a and 4b we compare the full results with the expansion approach at small quark mass values  $m = 180$  MeV in the case of the  $a_1$  and  $\rho$  mesons respectively. In the case of the  $\rho$ -meson the larger deviations observed between approximate and exact solutions at  $G_V > 12 \text{ GeV}^{-2}$  values stem from the fact that  $\text{Re}(z_\rho) < 1$ . In this region,  $12 < G_V < 20 \text{ GeV}^{-2}$ , the expansion curves interpolate between the resonance solutions and the bound state branch (if it exists). In Fig.4b we do not plot the bound state branch which starts at  $G_V = 20 \text{ GeV}^{-2}$ . As mentioned above, Eqs.(3) are not appropriate to describe resonance solutions in this region. The exact scalar resonances coincide with the ones obtained with the approximate ones (section 5) and are practically constant as functions of  $G_V$ .

**7.** As in ref.[6] we have studied here the resonance solutions in the extended NJL model in the quark–antiquark continuum. There is only one difference in our Lagrangian in comparison with that paper. We consider the model without the 't Hooft determinantal interaction. This interaction is important for solving the  $U(1)$  anomaly problem and, therefore, essential for the calculation of  $\eta - \eta'$  meson masses [13]. Since we restrict our consideration to the case of  $\rho$ ,  $a_1$  and  $\sigma$  mesons one can neglect these six quark vertices.



In any case, the results found in our study are independent of the precise form of the underlying NJL-type model. In ref.[6], the authors could not find the resonance solution in the case of the vector  $\rho$  meson. Instead, the “virtual state” has been found. In this letter we have studied this question more thoroughly. We have shown that the relativistic BS equation for the  $\rho$  meson state possesses also a resonance solution. This solution has a rather large imaginary part and corresponds to the physical  $\rho$  at small values of constituent quarks masses  $m \sim 200$  MeV. The imaginary part is a consequence of the deconfinement property of the NJL model and should be considered an artefact of the model. Nevertheless, the existence of resonance solutions is a very important feature of the model. It means in particular that the  $\rho$  meson state in the model exists as an asymptotic field and contributes at large time even at small values of  $m$ , although the probability for the detection of the particle decreases exponentially with a characteristic decay time  $\tau(\mathbf{p}) = \omega(\mathbf{p})/\gamma$ . The well-known Lagrangian (bosonization) approaches to the NJL model [8] use this fact without proof. An asymptotic  $\rho$  meson field is usually introduced in the bosonized NJL Lagrangian by the replacements of variables in the generating functional and finally, after the fixing of parameters, it happens often that the quark mass value is of the order of  $200 \div 300$  MeV. This procedure has a justification only if this state really exists in the model as a resonance in a quark–antiquark continuum. Our work proves for the first time this important fact.

**Acknowledgments** One of us (V.B.) would like to thank V. Branchina and J. Alexandre for useful discussions. It is a pleasure for A.B., B.H. and A.O. to thank E. van Beveren for stimulating discussions.

## References

- [1] Y. Nambu and G. Jona-Lasinio, Phys. Rev. 122 (1961) 345; 124 (1961) 246.
- [2] M. Takizawa, K. Tsushima, Y. Kohyama and K. Kubodera Nucl. Phys. A507 (1990) 611.
- [3] S. Klimt, M. Lutz, U. Vogl and W. Weise, Nucl. Phys. A516 (1990) 429; U. Vogl, M. Lutz, S. Klimt and W. Weise, Nucl. Phys. A516 (1990) 469; U. Vogl and W. Weise, Progress in Particle and Nuclear Physics Vol.26 (1990) 1.
- [4] A. H. Blin, B. Hiller and J. da Providência, Phys. Lett. B 241 (1990) 1.
- [5] E. M. Henley and H. Müther, Nucl. Phys. A 513 (1990) 667.
- [6] M. Takizawa, K. Kubodera and F. Myhrer, Phys. Lett. B 261 (1991) 221.
- [7] V. Bernard and Ulf-G.Meißner, Nucl. Phys. A489 (1988) 647.
- [8] J. Bijnens, Phys. Rep. 265 (1996) 369.
- [9] G. Höhler,  $\pi N$  Newsletter 7 (1992) 94, 9 (1993) 1.
- [10] V. Bernard, A. A. Osipov and Ulf-G.Meißner, Phys. Lett. B324 (1994) 201.

- [11] V. Bernard, A. H. Blin, B. Hiller, Yu. P. Ivanov, A. A. Osipov, and Ulf-G.Meißner, Ann. of Phys. (N.Y.) 249 (1996) 499.
- [12] W. Pauli and F. Villars, Rev. Mod. Phys. 21 (1949) 434.
- [13] V. Bernard, R.L. Jaffe and Ulf-G.Meißner, Nucl. Phys. B308 (1988) 753.

## Figure captions

Fig.1 Dependence of the real part  $\omega_\alpha$ , ( $\alpha = \rho$ , and  $a_1$ ) of the exact vector,  $\rho$ , and axial-vector,  $a_1$ , resonance solutions on  $G_V$  at large values of constituent quark masses  $m = 390$  MeV. The solid line corresponds to the bound state branch. It smoothly touches the  $q\bar{q}$  threshold line,  $2m$ . The dashed lines indicate resonance branches of  $\rho$  and  $a_1$  mesons. The dotted line is a “virtual-state” solution. The physical  $\rho$  is a bound state solution. The solid box indicates the region bounded by the values of a pion decay constant between  $f_\pi = 100$  MeV (left side of the box) and  $f_\pi = 92$  MeV (right side) where the physical  $\rho$  meson lies.

Fig.2 Same as Fig.1 for the small constituent quark mass  $m = 180$  MeV.

Fig.3 Comparison of the exact solutions (dashed lines) of the  $a_1$  meson BS equation for the quark mass  $m = 390$  MeV at different values of  $G_V$  with the corresponding solutions of the Eqs.(3) (dotted lines). Indicated is also the exact imaginary part  $\eta_\rho$  and  $f_\pi$ . For more details see text.

Fig.4 (a) Comparison of the exact solutions of the  $a_1$  meson BS equation for the quark mass  $m = 180$  MeV as functions of  $G_V$  with the corresponding solutions of the Eqs.(3), same notation as in Fig.3. (b) Same as (a) for the  $\rho$  meson. Indicated is also  $f_\pi$ .

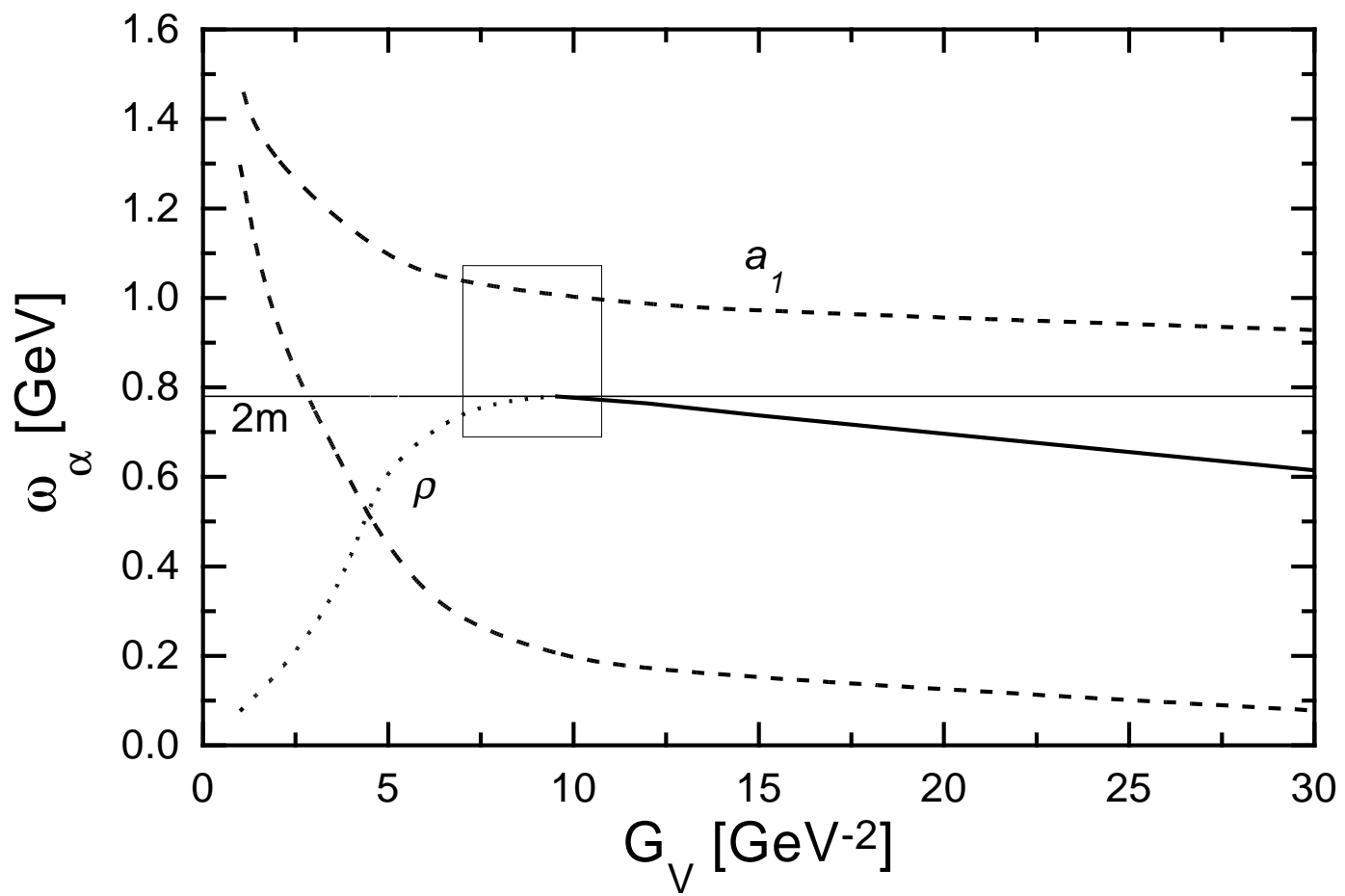


Figure 1

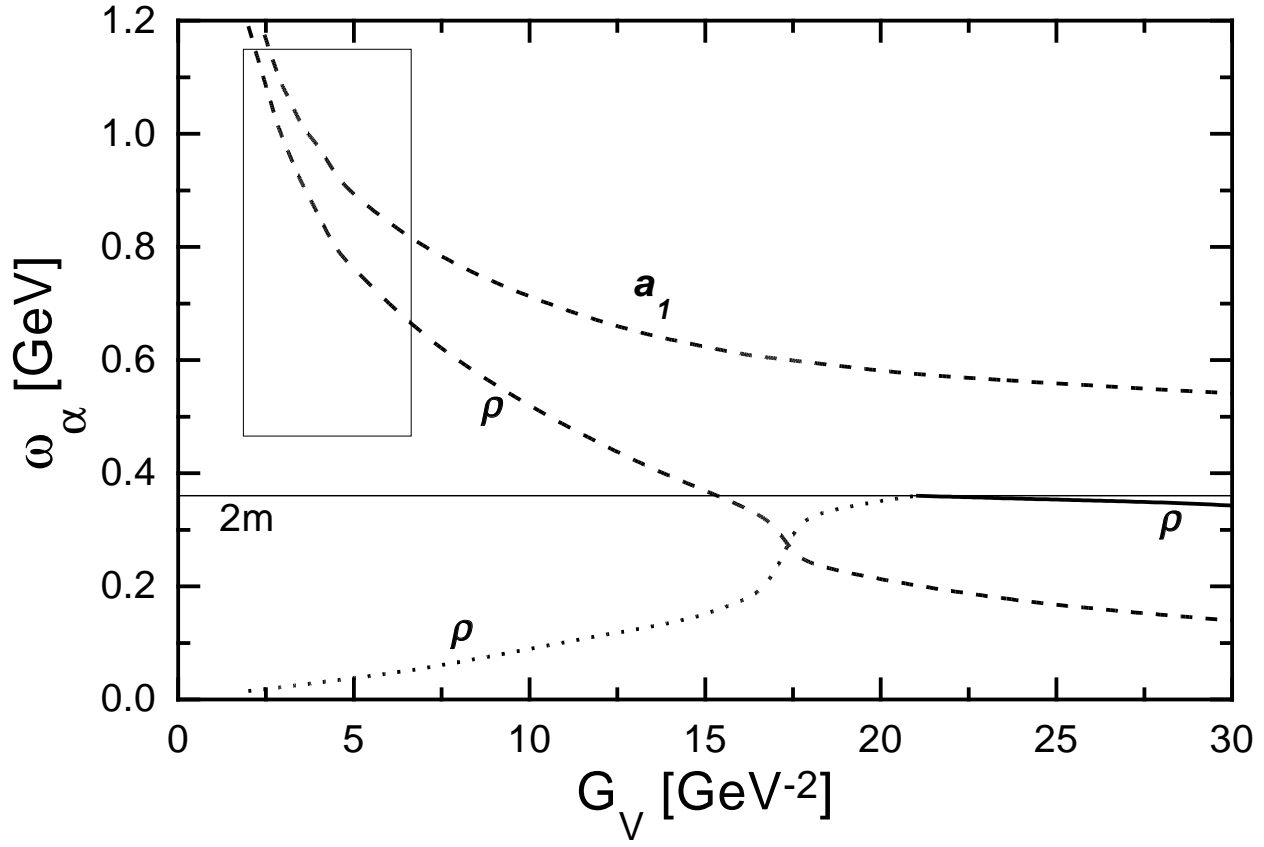


Figure 2

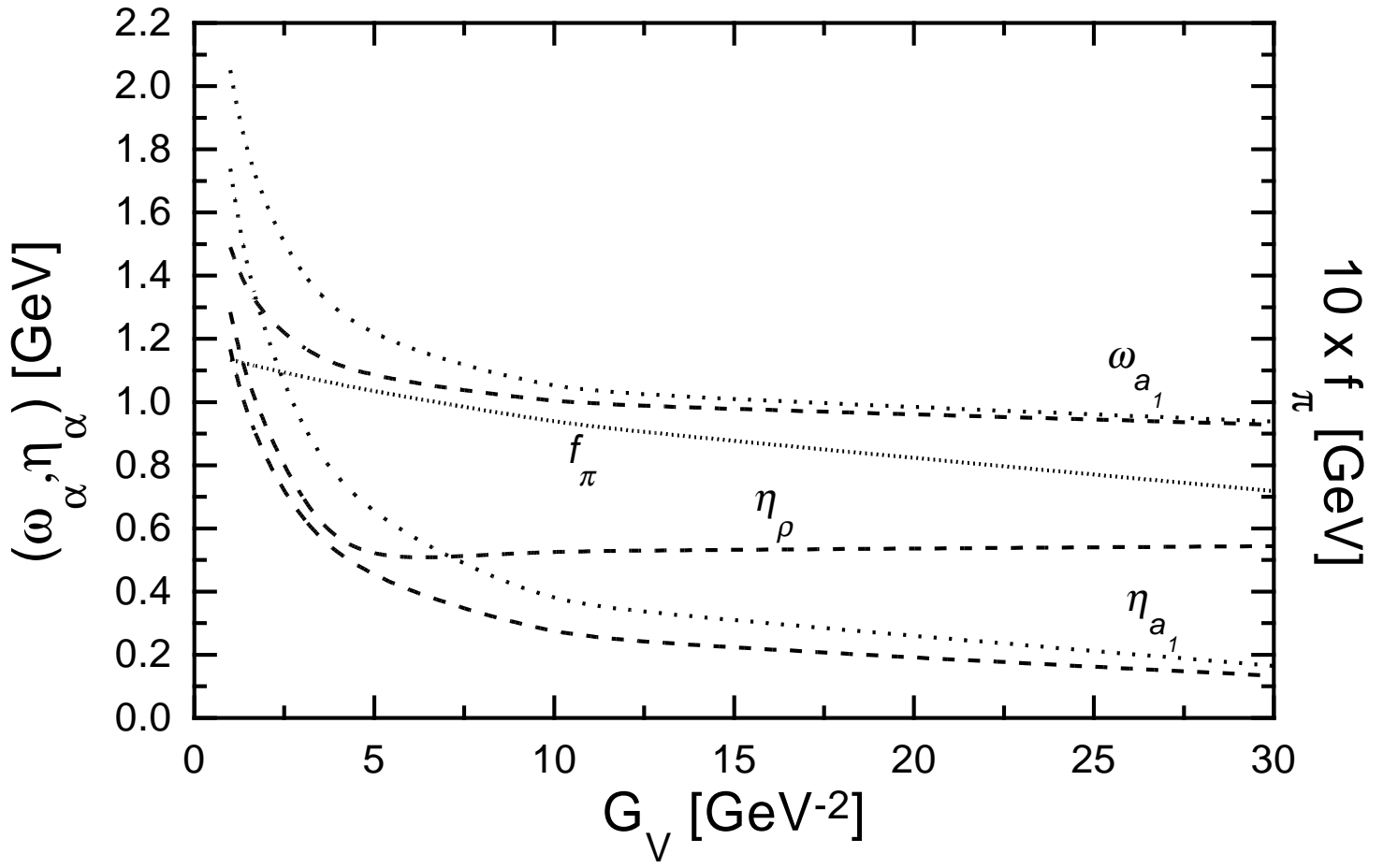


Figure 3

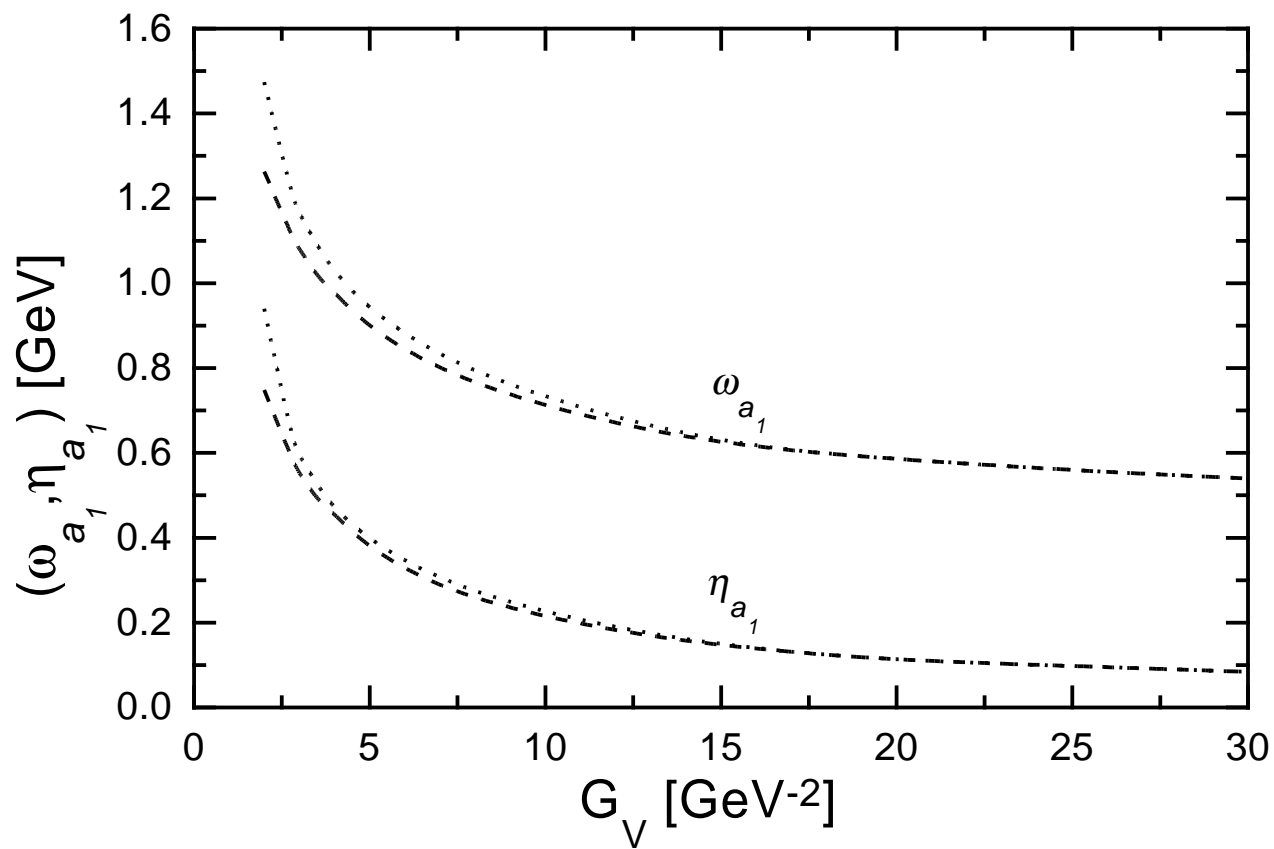


Figure 4a

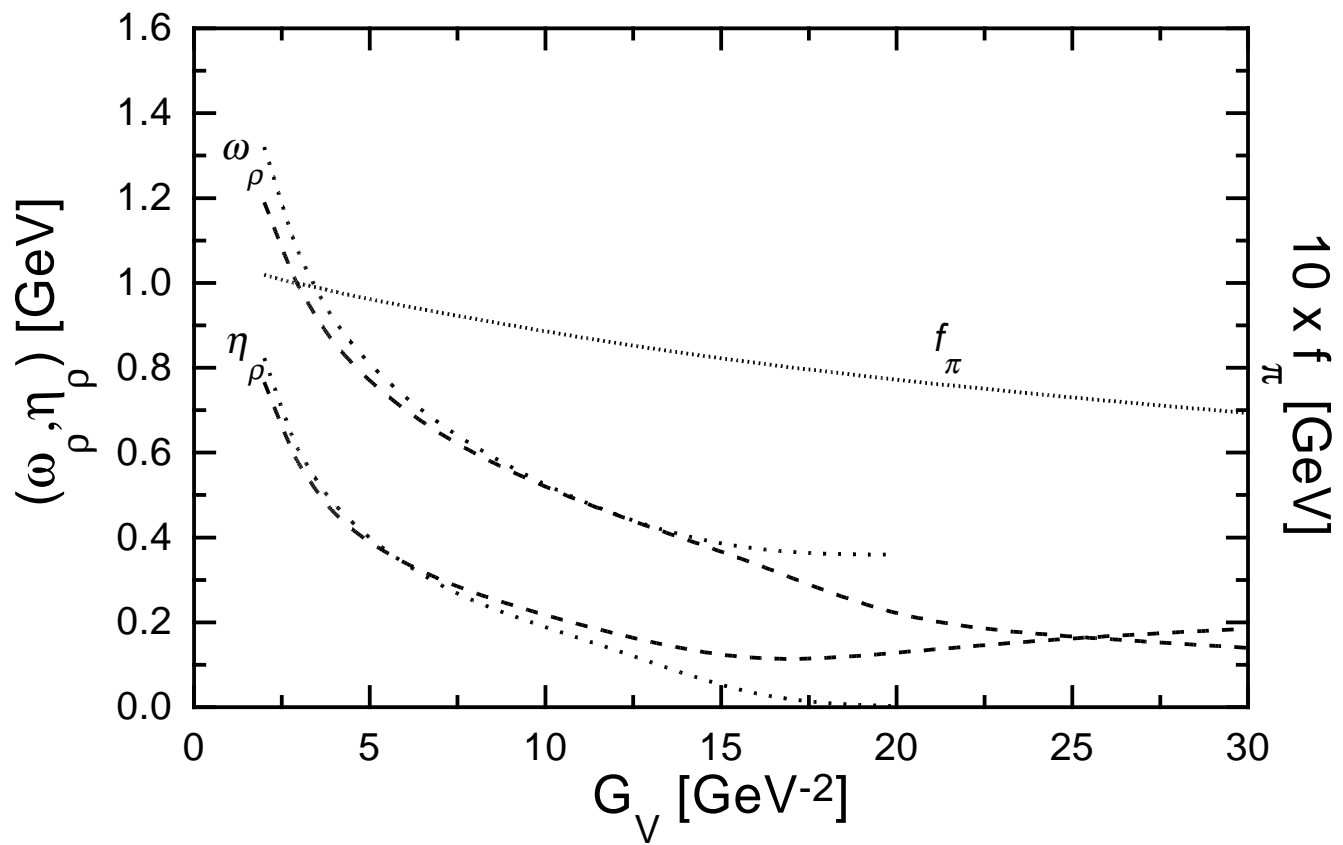


Figure 4b